BBA - Proteins and Proteomics xxx (xxxx) xxxx

Contents lists available at ScienceDirect

BBA - Proteins and Proteomics

journal homepage: www.elsevier.com/locate/bbapap

Constant domain-exchanged Fab enables specific light chain pairing in heterodimeric bispecific SEED-antibodies

Sylvia Dietrich[a,1], Alec W. Gross[b], Stefan Becker[c], Björn Hock[c,2], Gerhard Stadlmayr[d], Florian Rüker[d], Gordana Wozniak-Knopp[d,*]

[a] Christian Doppler Laboratory for Antibody Engineering, Department of Biotechnology, University of Natural Resources and Life Sciences, Vienna (BOKU), Muthgasse 18, 1190 Vienna, Austria
[b] Protein Engineering and Antibody Technologies, EMD Serono Research and Development Institute, Inc., 45A Middlesex Turnpike, Billerica, MA 01821, USA
[c] Protein Engineering and Antibody Technologies, Merck KGaA, Frankfurter Strasse 250, 64293 Darmstadt, Germany
[d] Christian Doppler Laboratory for Innovative Immunotherapeutics, Department of Biotechnology, University of Natural Resources and Life Sciences, Vienna (BOKU), Muthgasse 18, 1190 Vienna, Austria

ARTICLE INFO

Keywords:
Antibody chain association
Bispecific antibody
SEED antibody
Fab constant domain exchange
T cell redirection

ABSTRACT

Background: Bispecific antibodies promise to broadly expand the clinical utility of monoclonal antibody technology. Several approaches for heterodimerization of heavy chains have been established to produce antibodies with two different Fab arms, but promiscuous pairing of heavy and light chains remains a challenge for their manufacturing.

Methods: We have designed a solution in which the C_H1 and C_L domain pair in one of the Fab fragments is replaced with a C_H3-domain pair and heterodimerized to facilitate correct modified Fab-chain pairing in bispecific heterodimeric antibodies based on a strand-exchange engineered domain (SEED) scaffold with specificity for epithelial growth factor receptor and either CD3 or CD16 (FcγRIII).

Results: Bispecific antibodies retained binding to their target antigens and redirected primary T cells or NK cells to induce potent killing of target cells. All antibodies were expressed at a high yield in Expi293F cells, were detected as single sharp symmetrical peaks in size exclusion chromatography and retained high thermostability. Mass spectrometric analysis revealed specific heavy-to-light chain pairing for the bispecific SEED antibodies as well as for one-armed SEED antibodies co-expressed with two different competing light chains.

Conclusion: Incorporation of a constant domain-exchanged Fab fragment into a SEED antibody yields functional molecules with favorable biophysical properties.

General significance: Our results show that the novel engineered bispecific SEED antibody scaffold with an incorporated Fab fragment with C_H3-exchanged constant domains is a promising tool for the generation of complete heterodimeric bispecific antibodies with correct light chain pairing.

1. Introduction

Bispecific antibodies (BsAbs) incorporate two different binding specificities into a single molecule enabling new therapeutic modalities compared to classical monoclonal antibodies (mAbs) and are today together with antibody-drug conjugates the most intensely developing class of antibody-based therapeutics [1]. Examples of their unique mechanisms of action include disrupting signalling in tumor cells by

Abbreviations: ADCC, antibody-dependent cellular cytotoxicity; BiTE, Bispecific T-cell Engager; BsAb, bispecific antibody; CDC, complement-dependent cytotoxicity; CODV-Ig, cross-over dual variable immunoglobulin; DSC, differential scanning calorimetry; DVD-Ig, dual variable domain immunoglobulin; EGFR, epidermal growth factor receptor; EpCAM, epithelial cell adhesion molecule; Fab, fragment antigen binding; Fc, fragment crystallizable; FRET, Förster resonance energy transfer; HPLC, high pressure liquid chromatography; HTRF, homogeneous time resolved fluorescence resonance energy transfer; KiH, Knobs-into-Holes; LDH, lactate dehydrogenase; mAb, monoclonal antibody; MS, mass spectrometry; MW, molecular weight; NK cells, natural killer cells; PBMCs, peripheral blood mononuclear cells; PBS, phosphate buffered saline; SEC, size exclusion chromatography; SEED, Strand-Exchange Engineered Domain; TandAb, Tandem Antibody

* Corresponding author.
E-mail address: gordana.wozniak@boku.ac.at (G. Wozniak-Knopp).
[1] Current Affiliation: Agenus Inc., 3 Forbes Road, Lexington, MA 02421, USA.
[2] Current Affiliation: Biologics Technologies and Development, Ferring International Center S.A., Ch. de la Vergognausaz 50, CH-1162 Saint-Prex, Switzerland.

https://doi.org/10.1016/j.bbapap.2019.07.003
Received 18 March 2019; Received in revised form 13 June 2019; Accepted 3 July 2019

cross-linking mitogenic receptors [2], enhancing the selectivity for target cells by avid binding *via* moderate interaction with two cell-bound antigens [3], induction of receptor internalization caused by biparatopic binding [4], crossing of the blood–brain barrier, which makes them a therapeutic option in neurological diseases [5], and bridging of different cell types [6–8]. Their unique properties led to harvest of their therapeutic potential with regulatory approval for clinical use of first catumaxumab (anti-EpCAM x anti-CD3) in 2009 [9] and then blinatumomab (anti-CD19 x anti-CD3) in 2014 [1], both acting by recruiting immune cells for tumor eradication, followed by emicizumab (anti-activated factor IX x anti-factor X) in 2018, which mimics the function of the tenase complex mediated by activated factor VIII, deficient in people with haemophilia A [10].

Over the last three decades, antibody engineering led to a large variety of alternative BsAb formats with over 70 different now available, including Immunoglobulin G-like molecules, such as CrossMab [11], mAb^2 [12], DVD-Ig [13], CODV-Ig [14], assembled BsAbs [15,16], two-in-one antibodies [17] and Duetmabs [18], and several fusion proteins composed of an IgG and another antigen-binding molecule, but also immunoglobulin domain-based binding proteins without an Fc fragment such as TandAb and BiTE (reviewed recently in [19]). The current success of BsAbs is only possible because the initial limitations for their efficient production have been overcome, and the plethora of optimized formats allows for a choice of an optimal combination of antigen specificity and valency in a particular biological setting. An early prerequisite for developability of therapeutic bispecific antibodies is that the engineered proteins express at a high level, which favors the molecules with IgG-like architecture compatible with expression in a single cell or fermentor [20]. Random association of two wild-type heavy and light chains however leads to up to 10 different IgG species and the heterogenous mixture requires sophisticated downstream processing scheme and analytics.

The issue of random pairing of heavy chains was early solved by modifying C_H3 domains to promote heterodimerization of the two different heavy chains using either steric effects [21,22], electrostatic steering [23,24] or SEED technology [25], where the specific pairing of the C_H3 domains is achieved through their design of alternating segments from human IgA and IgG. Novel approaches involve driving heterodimerization by introducing amino acid residues present at the contact interface of the chains of naturally occurring heterodimeric molecules of immunoglobulin class [26]. Nevertheless, the pairing of heavy and light chains in two Fabs can still occur in a promiscuous way [27], adversely affecting antigen binding [28] and overall stability of the Fab fragment by altering the V_H/V_L packing [29]. Pairing propensity has been shown to follow certain rules [30,31] and pairing preferences do exist in the germline, but only for certain germline gene segments [32]. Several ingenious approaches have been designed to promote correct heavy-to-light chain association in bispecific antibodies to correctly reconstitute the different antigen binding sites (reviewed in [33]). An elegant solution is the combination of two antibodies of different specificities that share a common light chain [34–36], but methods for facile generation of suitable antibody candidates have only been demonstrated recently [37]. Correct assembly of four different chains with only a small fraction of side products was described for a CrossMab molecule [11], in which correct heavy chain pairing is achieved by “Knobs-into-holes”(KiH) technology and specific light chain pairing by domain crossover technology in one of the two Fab fragments. Other approaches to promote specific heavy-to-light chain pairing involved introducing steric or electrostatic effects by mutagenesis of residues at the contact points of V_H/V_L [38], C_H1/C_L [39] or both V_H/V_L and C_H1/C_L [40,41].

In this work, we describe the generation and characterization of novel IgG-like BsAbs by combining two engineering technologies: SEED technology [25] for heterodimerization of two different heavy chains, and the recently described replacement of the C_H1/C_L domains with an IgG1 C_H3 domain pair for correct heavy-to-light chain pairing [42]. We selected SEED technology because of the positive therapeutic assessment that included evaluation of biochemical and biophysical properties of the resulting molecules, its versatile compatibility with different combinations of Fab, scFv and V_{HH} domains, and antibody-like biological functionality of the SEED-Fc [43]. Two BsAbs with specificity for EGFR and either CD3 or CD16, were designed in this way and produced at a high yield as highly homogenous heterodimeric molecules by co-expression of four chains in mammalian cells. The resulting proteins showed a single sharp symmetrical peak when eluted in HPLC in native conditions and maintained high thermostability. These BsAbs retained full binding to both of their respective cognate antigens, and armed human immune effector cells to potently induce lysis of target cells. Our results show that this format is a promising tool for the generation of BsAbs combining two different binding specificities in a single molecule.

2. Material and methods

2.1. Gene synthesis, expression and purification of antibodies

DNA sequences of the variable domains of used antibodies were synthesized by GeneArt (Life Technologies). C_H3 sequences for constant domain exchange were mutagenized using Quickchange Lightning Mutagenesis kit (Agilent Technologies). Nucleotide sequences encoding antibody domains were PCR-amplified with oligonucleotides containing flanking restriction sites to allow cloning of complete antibody chains (Supplementary Table 1) into pTT5 expression vectors (CNRC).

Proteins were produced by transient transfection of Expi293F using the ExpiFectamine™ 293 Transfection Kit (Thermo Fisher) following the procedures recommended by the supplier. The expression of complete antibodies was accomplished by co-transfection of selected combinations of vectors. For each 30-mL-transfection, 7.5×10^7 cells were resuspended in 25.5 mL of Expi293™ Expression medium and transferred to a 125 mL-Erlenmeyer flask. For the preparation of the lipid-DNA complexes, 30 µg of plasmid DNA were gently mixed in Opti-MEM®I Reduced Serum Medium (Thermo Fisher) in a total volume of 1.5 mL and 81 µL of ExpiFectamine™ 293 Reagent were added to 1.5 mL of Opti-MEM®I Medium. After incubating for 5 min at room temperature (RT), the diluted DNA was added to the diluted ExpiFectamine™ 293 Reagent, gently mixed and incubated for additional 20 min at RT. The 3 mL lipid-DNA complex was added to each flask and incubated for 18 h at 37 °C and 8% CO_2 on a shaking platform. 150 µL of ExpiFectamine™ 293 Transfection Enhancer 1 and 1.5 mL of ExpiFectamine™ 293 Transfection Enhancer 2 were added. 6 days after transfection, cell culture medium was collected, sterile filtered and incubated in batch mode with ProSep Ultra Plus Protein A Resin (Merck Millipore) for 1 h at RT with constant low speed shaking to prevent resin settlement. After elution, proteins were buffer exchanged into PBS using PD-10 Desalting Columns (GE Healthcare).

2.2. Preparative SEC-HPLC

Preparative SEC purification was performed on an Äkta Purifier (GE Healthcare) using a Superdex 200 10/300 GL column (GE Healthcare) equilibrated with PBS (Thermo Fisher). Proteins were eluted with isocratic flow of 1 mL/min and collected in 1 mL aliquots in 96-well plates.

2.3. Analytical SEC-HPLC

One-armed antibodies were analyzed on LC-20A Prominence system (Shimadzu) with a *Superdex* 200 Increase 10/300 GL column (GE Healthcare). The mobile-phase buffer used was PBS with 200 mM NaCl. Chromatography was conducted with a constant flow rate of 0.75 mL/min. A total of 50 µg protein at about 1 mg/mL were loaded on the column for analysis. Column calibration was performed with a set of molecular weight (MW) standards ranging from 10 to 500 kDa (Bio-

Rad).

Protein samples were analyzed on a 1260 Infinity LC Systems (Agilent Technologies) with sample concentrations between 0.5 and 1 mg/mL. Before loading, the TSK-GEL Super SW3000 SEC column 4.6 × 300 mm (Tosoh Biosciences) was equilibrated with 50 mM sodium phosphate, 400 mM sodium perchlorate, pH 6.3 ± 0.1. Peak values were determined using Empower Software (Waters Corp., Milford, MA, USA).

2.4. SDS-PAGE

The purity of purified protein samples was analyzed using SDS-PAGE analysis in reducing and non-reducing conditions. Samples were diluted to a final concentration of 0.25 mg/mL with NuPAGE LDS Sample Buffer (Thermo Fisher) containing 1 mM maleimide Solution (Sigma-Aldrich) for analysis in non-reducing conditions or NuPAGE Sample Reducing Agent (Thermo Fisher) for analysis in reducing conditions. Samples were heated at 85 °C for 4 min and 5 µg of protein were loaded onto NuPAGE® 4–12% Bis-Tris Gel (Thermo Fisher). Electrophoresis was run in NuPAGE® MOPS SDS Running Buffer (Thermo Fisher) at 200 V for 50 min for the non-reduced samples and NuPAGE® MES SDS Running Buffer (Thermo Fisher) at 200 V for 35 min for the reduced samples. Gels were stained using Colloidal Blue Staining Kit (Thermo Fisher), destained with distilled water and scanned using ImageQuant LAS 4000 Imager (GE Healthcare).

2.5. MS analysis

Antibody samples (~20 µg) in distilled water were dried in vacuum, dissolved in 50 µL 50 mM ammonium acetate (pH 8.4) and treated with 1 U PNGaseF (Roche) at 37 °C for 16 h. 5 µl of each antibody sample were used for the analysis by LC-MS in a gradient from 25 to 80% acetonitrile within 15 min on a ProSwift RP-4H column (250 mm*0.2 mm) (Thermo Fisher). Detection of proteins was performed on a Bruker maXis 4G Q-TOF (0.3 Hz spectrum rate, 200 ms transfer time, 20 µs pre pulse storage, 150 eV isCID). Deconvolution of summed spectra was done using the MaxEnt algorithm in Data Analysis 4.0.

2.6. DSC

Protein samples (0.5 µg in total) were buffer-exchanged into PBS, pH 7.4 (Thermo Fisher) using the PD10 Desalting Columns (GE Healthcare) according to the manufacturer's instructions. The concentration of the proteins was adjusted to 0.1 to 0.2 mg/mL. Samples and buffer were degassed under vacuum for at least 30 min before measurement. Proteins were loaded into a VP-DSC microcalorimeter (GE Healthcare) and measured with a scanning rate of 1.5 °C/min from 15 °C to 95 °C. Data were analyzed using Origin 7.0. PBS buffer baseline was subtracted, and data were normalized to the molar concentration of the protein. Fitting was performed using the non-2-state model.

2.7. Cell lines and culture

EGFR-positive A431 cells (ATCC® CRL-1555) were cultured in RPMI 1640 medium (Thermo Fisher), supplemented with heat-inactivated 10% FBS (Thermo Fisher) in a humidified atmosphere with 5% CO_2 at 37 °C. For flow cytometry experiments, cells were detached with TrypLE™ Express Enzyme (Thermo Fisher) and live cells after Trypan Blue exclusion were counted using Countess™ Automated Cell Counter (Thermo Fisher). For the cytotoxicity assays, target cells were co-cultured with effector cells in RPMI 1640 phenol red-free medium (Thermo Fisher) supplemented with heat-inactivated 0.5% FBS in a humidified atmosphere with 5% CO_2 at 37 °C for 16 h.

2.8. Preparation of human PBMCs

Human peripheral blood mononuclear cells (PBMCs) were prepared from human blood samples using Ficoll density centrifugation. The blood samples were diluted with an equal volume of PBS and 25 mL of diluted samples were layered on 15 mL of Ficoll-Paque PLUS (GE Healthcare). After centrifugation at RT and 900 *g* for 30 min with brake off, the PBMCs in the interface were collected and washed twice with PBS at 900 g for 5 min. Cells were counted using the Countess™ Automated Cell Counter (Thermo Fisher).

2.9. T cell and NK cell isolation

Primary T-cells or human NK cells were isolated from PBMCs using Pan T cell Isolation Kit, human (Miltenyi Biotech) or NK cell Isolation Kit, human (Miltenyi Biotech) according to the manufacturer's instructions. Briefly, 2×10^8 fresh isolated PBMCs were resuspended in 800 µL of autoMACS Running Buffer and 200 µL of Biotin-Antibody Cocktail. The cell-antibody mixture was incubated for 5 min in the refrigerator (2–8 °C). To label the non-target cell with the magnetic beads, 600 µL of autoMACS Running Buffer and 400 µL of MicroBead Cocktail was added and incubated for an additional 10 min in the refrigerator (2–8 °C). Magnetic separation of labeled and un-labeled cells was performed by the autoMACS Pro Separator (Miltenyi Biotech) using the program 'Depletes'. Non-stimulated T cells and NK cells were cultivated in RPMI 1640 medium supplemented with 10% heat-inactivated FBS for 24 h before use in cytotoxicity assay.

2.10. T cell stimulation

A 75 cm^2 culture flask was coated with 10 µg/mL of anti-CD3 OKT3 antibody in PBS for 90 min at 37 °C. A total of 2×10^7 isolated PBMCs were resuspended in 10 mL RPMI 1640 medium supplemented with 10% heat-inactivated FBS containing 30 U/mL IL-2 (R&D Systems) and activated on the coated plate in humidified atmosphere with 5% CO_2 for 24 h at 37 °C.

2.11. Cell binding

A431 cells and primary T cells were blocked with 2% BSA-PBS on ice for 30 min. Antibodies were added in 3-fold serial dilution in 2% BSA-PBS, incubated on ice for 30 min, and binding was detected using an anti-human Fc $F(ab)_2$ antibody conjugated with phycoerythrin (Sigma-Aldrich) in 1:800 dilution in 2% BSA-PBS on ice for 30 min. Measurements of fluorescence of the cell population were performed in duplicates on a Guava® easyCyte flow cytometer (Merck Millipore).

Cell binding of BsAb2 to the CD16a receptor was measured using a CD16a HTRF cellular binding assay, using HEK293 cells that express the CD16a receptor with the functionally relevant gamma chain labeled with Terbium donor dye. In the assay, unlabelled antibodies compete with an acceptor-labeled human IgG for binding to the receptor. The cells were thawed, washed with PBS at 300 g for 5 min at RT, resuspended in Tag-lite buffer and distributed to the microtiter plate wells. 3-fold serial dilution of antibodies in Tag-lite buffer were added in duplicates. Finally, a solution of the labeled IgG (IgG-2d) was added. Incubation was for 2 h at RT and fluorescence was read at 665/615 nm on Molecular Devices SpectroMax M5 microplate reader.

2.12. Cytotoxicity assay

All cytotoxicity assays were performed with EGFR-positive A431 cells as target cell. Isolated T cells with or without previous stimulation or NK cells were used as effector cells depending on the bispecific antibody tested. Target and effector cells were co-incubated in 96-well round-bottom plates at an effector to target (E:T) ratio of 10:1 with a final defined number of 2×10^5 target cells per well. Test antibodies

were added to the cells in 4-fold dilutions to a total volume of 200 µL and the incubation proceeded for 4 h for NK cells and 18 h for activated T cells in a humidified atmosphere with 5% CO_2 at 37 °C. Cells were then collected by centrifugation and the supernatant was used for lactate dehydrogenase (LDH) release measurement with CytoTox96® Non-Radioactive Cytotoxicity Assay (Promega) according to the manufacturer's instructions. Percentages of specific lysis were calculated according to the formula: % cytotoxicity = [(experimental release)—(effector spontaneous release)—(target spontaneous release)] / [(target maximum release)—(target spontaneous release)] x 100.

3. Results

3.1. Design of bispecific antibodies

Heterodimerization of the two different heavy chains was performed using SEED technology [25]. To achieve correct heavy-to-light chain pairing and reduce the fraction of undesired side products in the bispecific antibody preparation (Fig. 1A), we have engineered one of the two Fab interfaces by exchanging the C_H1/C_L domains of the Fab with paired C_H3 domains, following engineering principles described recently [42]. Namely, the paired C_H3 domains exchanged into the Fab in place of the C_H1/C_L domains are a structurally similar immunoglobulin domain as the Fab constant domains they replace and mediate C_H3-to-C_H3 domain protein-protein interactions. To increase the specificity of the exchanged domain interactions, the exchanged C_H3 domain pairs incorporate" KiH" motif, which was chosen for the study due to the minimal number of amino acid substitutions required to drive an efficient C_H3 domain heterodimerization. Furthermore, the last three C-terminal residues of the newly introduced C_H3 domains were modified into amino acids –KSC in the heavy chain and –GEC in the light chain elements of the Domain-Exchanged Fab, to allow formation of a disulfide bond analogous to the one present natively between heavy chain and light chain in the unmodified Fab fragment [42,44] (amino acid sequences of all constructs are given in Supplementary Table 1).

Schematic depiction of the protein design is shown in Fig. 1B. The wild-type Fab in our constructs is composed of the light chain (V_L1-C_L) and the Fd fragment (V_H1-C_H1) of the unmodified Fab of the first antibody, which is fused to the GA chain of the SEED-Fc fragment to form the N- to C-terminal sequence of domains: V_H1-C_H1-C_H2-$C_H3_{SEED\text{-}GA}$ (combinations of transfected chains for all constructs are given in Supplementary Table 2). The variable domain of the light chain of the second antibody incorporated into the Domain-Exchanged Fab is fused to the "Hole" variant of the C_H3 domain with the mutation Y407T (EU numbering scheme) [45] (V_L2-C_H3_H). The variable domain of its heavy chain is fused to the "Knob" variant of the C_H3 domain with the mutation T366Y, and continues into the AG-chain of the SEED variant of the Fc fragment to give the sequence of domains V_H2-C_H3_K-C_H2-$C_H3_{SEED\text{-}AG}$ as the AG chain is less likely to homodimerize than GA [25]. The "Knob" variant of the newly introduced C_H3 domains was chosen for the heavy chain element, as it reportedly obstructs homodimerization more efficiently than the "Hole" mutation [21,46], and thus may reduce unwanted domain interactions and chain assembly during cellular production. However, it is worth noting that efficient correct heavy-to-light chain pairing can also be achieved without additional introduction of the "Knobs-into-holes" substitutions.

3.2. Model antibodies

We aimed to produce bispecific SEED antibodies with the ability to trigger redirected effector cell killing of tumor cells. For target cell binding, we chose the variable regions of the humanized antibody hu425 (matuzumab) [47], which binds to the epithelial tumor marker EGFR. Target cell lysis mediated through T cell binding and activation should be efficiently promoted by the murine CD3-targeting OKT3 antibody (Muromonab-CD3) [48,49], or by the murine anti-CD16 3G8 antibody [50], when NK cells are used as effector cells.

To evaluate the feasibility of combining Domain-Exchanged Fabs with the SEED heavy chain heterodimerization technology, we constructed and purified unmodified Fab and Domain-Exchanged Fab one-armed SEED antibodies (Fig. 2) for each individual candidate (variable domains are designated $V_{H/L}$hu425, $V_{H/L}$OKT3 and $V_{H/L}$3G8). The analysis of protein preparations after Protein A purification and analytical gel filtration with SEC-HPLC in native conditions resulted in > 95% protein corresponding to the size of parental one-armed SEED antibody with variable domains of all three antibodies, without detectable fragments of lower MW.

3.3. Antibody generation and biophysical characterization

Two bispecific SEED antibodies BsAb1 (anti-EGFR x anti-CD3) and BsAb2 (anti-EGFR x anti-CD16) were produced using transient expression in Expi293F suspension cells with co-transfection of four expression plasmids at optimized plasmid ratios. Both BsAbs were purified by standard Protein A purification followed by preparative SEC at a yield

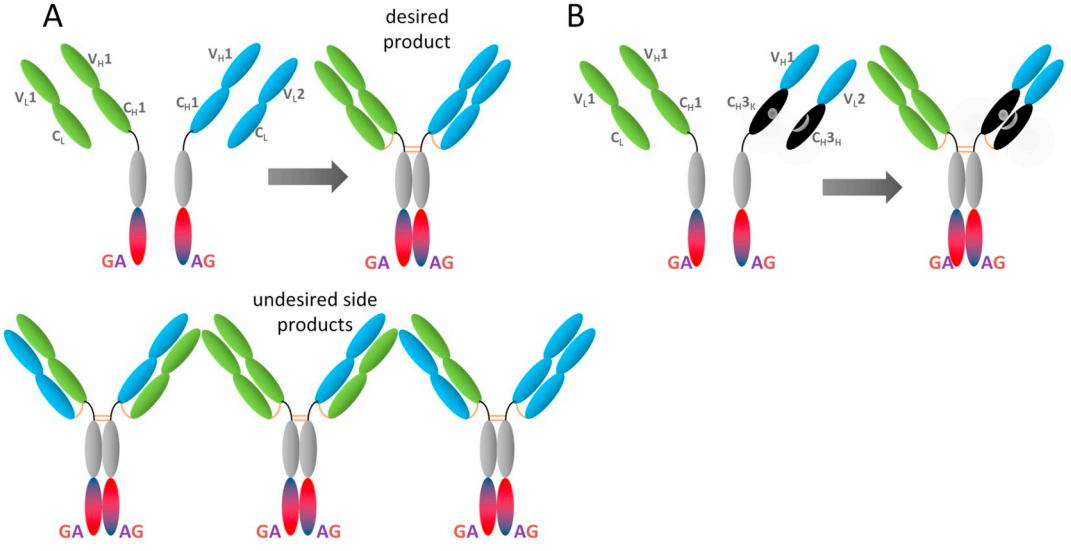

Fig. 1. (A) Bispecific SEED antibodies expressed with two heavy and two light chains and the possible resulting products; (B) Design of domain-exchanged bispecific C_H3_{KiH} SEED antibody.

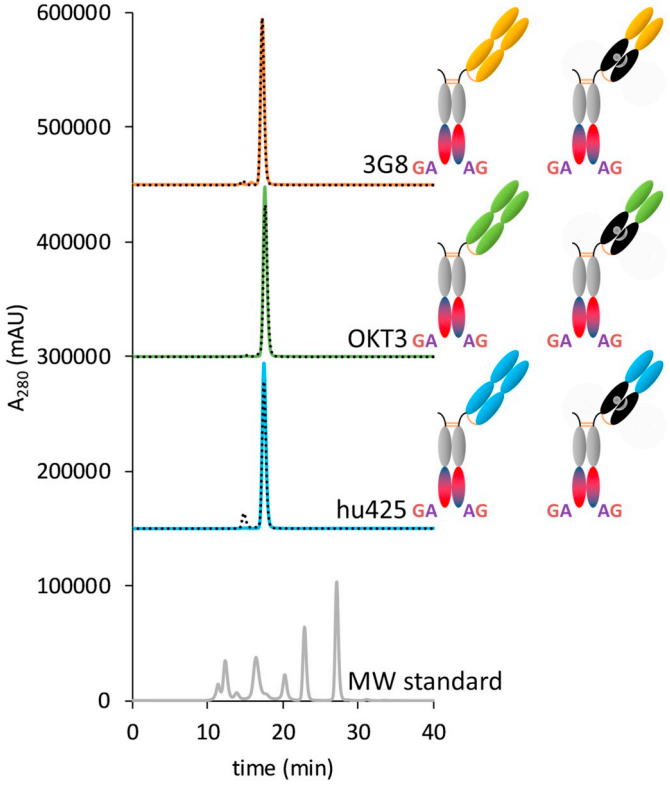

Fig. 2. SEC-HPLC profiles of one-armed C_H1/C_L SEED antibodies (full line) and C_H3 SEED antibodies (dotted line) hu425, OKT3 and 3G8 after Protein A purification and subsequent gel filtration. Gray line: gel filtration standard was the mix of protein size indicators of 670, 158, 44, 17 and 1.35 kDa (Bio-Rad).

of up to 200 mg/L and characterized for their biophysical properties.

SDS-PAGE analysis of Protein A-purified preparations of BsAb1 and BsAb2 in non-reducing conditions showed a single predominant band with a MW of ~150 kDa, corresponding to the properly assembled disulfide-bridged antibody (HC_2LC_2) (Fig. 3A). Additional minor bands were detected at a size of ~125 kDa, likely corresponding to BsAbs lacking one light chain (HC_2LC), ~100 kDa, which could be a heavy chain dimer (HC_2), ~75 kDa, which could correspond to a half of the antibody molecule (HCLC), and the ~23 kDa band, corresponding to free LC molecules. The putative proteins detected as minor bands could result from incomplete inter-chain disulfide bond formation at different positions of the proteins, which then separate under non-reducing SDS-PAGE conditions due to the presence of detergent. Alternatively, fragmentation of antibodies to produce minor bands in non-reducing SDS-PAGE can occur as gel artifacts. Under reducing conditions, the larger MW bands of BsAb1 and BsAb2 all reduced in size, as expected. Three main bands for BsAb1 and four bands for the BsAb2 were detected. For both BsAbs, the two different heavy chains HC1 and HC2 could be separated to individual protein bands. The upper band HC2 of the doublet corresponds to the domain-exchanged $V_H$hu425-C_H3_K-C_H2-$C_H3_{SEED\text{-}AG}$ chain with calculated MW of 51.5 kDa for both BsAbs. The lower band HC1 corresponds to the V_HOKT3-C_H1-C_H2-$C_H3_{SEED\text{-}GA}$ chain with calculated MW of 50 kDa for BsAb1 and the analogous V_H3G8-C_H1-C_H2-$C_H3_{SEED\text{-}GA}$ chain with calculated MW of 49.5 kDa for BsAb2. The two chains with light variable domains, V_LOKT3-C_L and $V_L$hu425-C_H3_H of BsAb1 appeared as a single band of about ~25 kDa in size (calculated MW of 23.3 kDa and 23.7 kDa, respectively). The V_L3G8-C_L and $V_L$hu425-C_H3_H of BsAb2 were separated into two individual bands (calculated MW of 23.7 kDa and 23.7 kDa, respectively).

The BsAbs were further characterized by analytical SEC-HPLC. After gel filtration, a predominant peak with an area of 99% for BsAb1 and 95% for BsAb2, eluting at a time corresponding to a properly assembled antibody, was detected for both tested samples (Fig. 3B). BsAb1 was free of aggregates and degradation products, while for the preparations of BsAb2 two minor additional peaks were detected, one of higher and one of a lower MW than the main peak. The detection of one main peak for BsAb1 and BsAb2 by analytical SEC-HPLC suggests that in solution there was primarily one protein corresponding to the MW of a bivalent antibody. Thus proteins representing the minor bands separated in non-reducing SDS-PAGE after heating in buffer with detergent were not detected by SEC-HPLC in solution. Together, these results suggest efficient assembly of BsAbs with 4 protein chains in an IgG-like format.

To analyze in detail the assembly of the 4 co-expressed protein chains in the BsAbs, a more sensitive and precise analysis using mass spectrometry was required. Purified BsAb1 and BsAb2 (protein A and preparative SEC purified) were de-glycosylated by treatment with PNGaseF and their mass measured by LC-MS (Fig. 4A and B). The mass of BsAb1 was 148,284 Da and the mass of BsAb2 was 148,050 Da. Compared to the calculated average mass expected from the correct assembly of the BsAb design as depicted in Fig. 1B, the actual measured average mass differed by only < 4 Da for BsAb1 and ~12 Da for BsAb2.

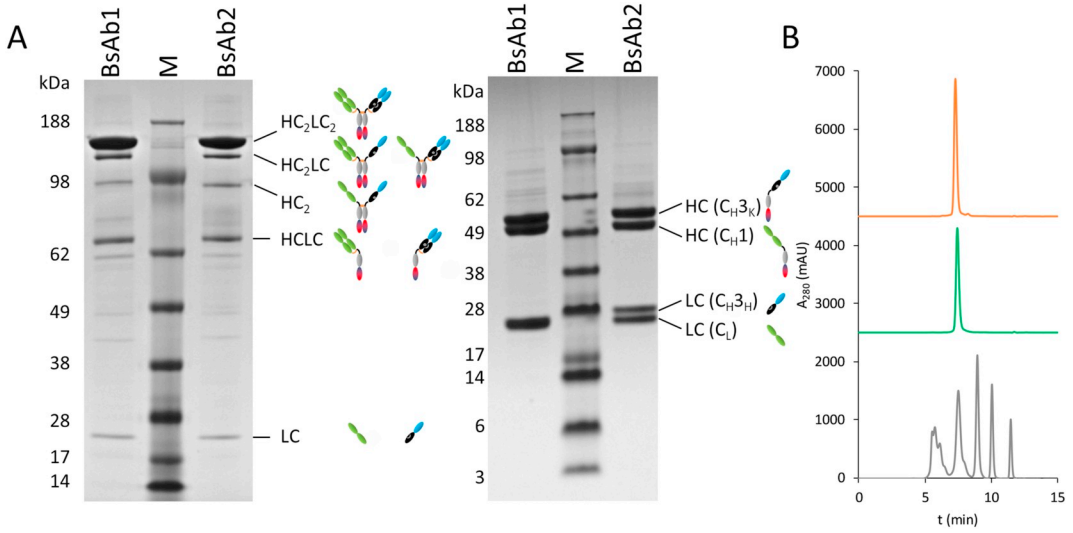

Fig. 3. (A) SDS–PAGE of bispecific SEED antibodies BsAb1and BsAb2. M: See Blue Plus 2 Pre-Stained Molecular Weight Marker (Thermo Fisher); (B) Analytical SEC-HPLC chromatograms of the bispecific SEED antibodies BsAb1 (green) and BsAb2 (orange), purified with Protein A and preparative SEC, gel filtration standard was the mix of protein size indicators of 670, 158, 44, 17 and 1.35 kDa (Bio-Rad) (gray).

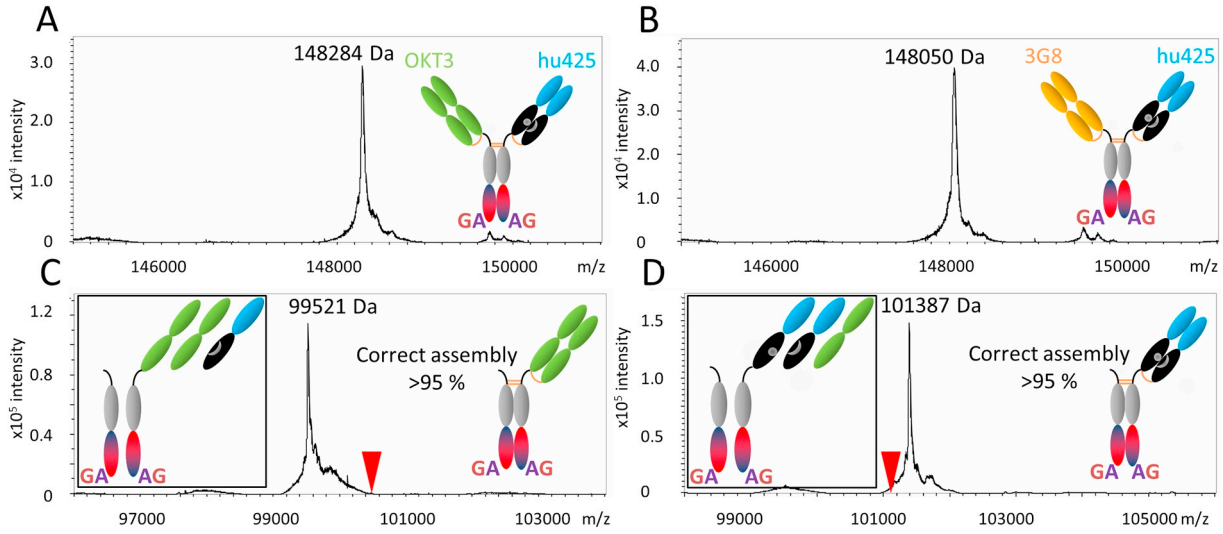

Fig. 4. LC-MS analysis of BsAbs. (A) Deconvoluted sum spectrum shows the mass of correctly assembled BsAb1 and (B) mass of correctly assembled BsAb2. The outcome of competition experiments where both $V_L$hu425-C_H3_H and V_LOKT3-C_L light chains were co-expressed with one-armed SEED antibody heavy chain elements (boxed diagrams) to test the potential for incorrect heavy-to-light chain pairing was: (C) correctly assembled one-armed OKT3-C_H1/C_L SEED antibody and (D) correctly assembled one armed hu425-C_H3_{KiH} SEED antibody. Red arrows indicate the expected position of the incorrect heavy and light chain pairs.

Thus, MS analysis demonstrated that the 4 co-expressed protein chains were assembled in BsAb1 and BsAb2 with the expected stoichiometry of 1 of each of the 4 protein chains per molecule.

However, this mass spectrometry analysis could not distinguish if each light chain was correctly paired with its matching heavy chain in the BsAbs, or if it was possible for light chain elements of the BsAb to incorrectly pair with the heavy chains (which would still result in the same measured 1:1:1:1 stoichiometry of the 4 protein chains). Therefore, to conduct a sensitive test of the potential for promiscuous light chain pairing among the unmodified Fab elements and Domain-Exchanged Fab elements in our BsAb design (Fig. 1B), a co-expression competition assay was performed. Both light chains from BsAb1 were co-expressed with just one of the heavy chains of BsAb1 in the format of a one-armed antibody with Fab heavy chain elements fused to the AG chain of the SEED-Fc (Fig. 4C and D). Separate competition assays were performed, with both BsAb1 light chains competing for assembly with each of the BsAb1 heavy chain elements, one-heavy-chain-at-a-time. After Protein A purification and de-glycosylation, the one-armed antibodies that resulted were detected by MS (Fig. 4C and D).

Fig. 4C shows the result of competition between unmodified light chain (V_LOKT3-C_L) and Domain-Exchanged light chain ($V_L$hu425-C_H3_H) for assembly onto unmodified heavy chain (V_HOKT3-C_H1-C_H2-$C_H3_{SEED-AG}$) as a one-armed antibody. MS detected protein with the mass of the correctly assembled one-armed anti-CD3 OKT3-SEED antibody (99,521 Da). No mispaired one-armed antibody assembled with the incorrect light chain was detected. Based on the estimated detection limit for mispaired one-armed antibody, it can be stated that > 95% of the one-armed antibody assembled with the correct light chain.

Fig. 4D shows the result of competition between unmodified light chain (V_LOKT3-C_L) and Domain-Exchanged light chain ($V_L$hu425-C_H3_H) for assembly onto domain-exchanged heavy chain ($V_H$hu425-C_H3_K-C_H2-$C_H3_{SEED-AG}$) as a one-armed antibody. MS detected protein with the mass of the correctly assembled one-armed anti-EGFR hu425-SEED antibody (101,387 Da). No mispaired one-armed antibody assembled with the incorrect light chain was detected. Again, based on the estimated detection limit for mispaired one-armed antibody, it can be stated that > 95% of the one-armed antibody assembled with the correct light chain.

These co-expression competition assays demonstrated very specific assembly, as intended, of the matching light chain and heavy chain elements. The unmodified light chain was only seen to assemble with the unmodified heavy chain Fab element, and the Domain-Exchanged light chain was only seen to assemble with the Domain-Exchanged heavy chain Fab element. Together with the 1:1:1:1 protein chain stoichiometry determined by MS of the full BsAb1 and BsAb2 proteins, these sensitive and precise MS analyses strongly suggest efficient and accurate assembly of the 4 co-expressed protein chains occurs as diagrammed in Fig. 1B, and that including Domain-Exchanged Fab elements in the BsAb successfully drives correct heavy-to-light chain pairing.

After determining that BsAb1 and BsAb2 were correctly assembled, we went on to test the stability of these proteins. We measured the thermal stability of BsAb1 and BsAb2 with differential scanning calorimetry (DSC) (Fig. 5). Endotherms measured for BsAb1 and BsAb2 were compared to those of one-arm anti-EGFR SEED antibody variants to aid deconvolution of the thermal unfolding profiles of the multi-domain proteins and assign the melting temperatures to separate melting events. Further, the endotherm of the one-armed anti-EGFR SEED antibody was compared to that recorded for the Domain-Exchanged version of one-armed anti-EGFR SEED antibody to illustrate the effect of this particular modification.

The bivalent anti-EGFR C_H1/C_L SEED antibody unfolded with two well separated transitions, one at T_m = 68.9 °C and a second at T_m = 75.1 °C. Based on published results, the first transition can be assigned to melting of the SEED-Fc fragment and the second one to melting of the Fab fragment [43]. The transitions observed for the monovalent anti-EGFR C_H1/C_L SEED antibody matched the ones observed for the bivalent anti-EGFR IgG, except as expected the area for the hu425 Fab peak was smaller since there was only 1 Fab per molecule instead of 2 Fabs per molecule (Fig. 5).

The one-armed Domain-Exchanged anti-EGFR antibody displayed a different unfolding profile compared to the one-armed antibody with unmodified Fab. The thermal denaturation of the SEED-Fc domain occurred at T_m = 66.4 °C and overlapped with the thermal denaturation of SEED domains of the bivalent and one-armed anti-EGFR antibodies. Thermal denaturation of the Domain-Exchanged Fab however occurred at T_m = 61.4 °C, a lower temperature than that determined for the unmodified Fab fragment.

Both bivalent BsAbs endotherms when deconvoluted fit to show they unfolded with three transitions. The first transitions of BsAb1 and BsAb2 were observed at T_m = 61.7 °C and T_m = 61.3 °C, respectively. This transition corresponds to the thermal unfolding of the Domain-

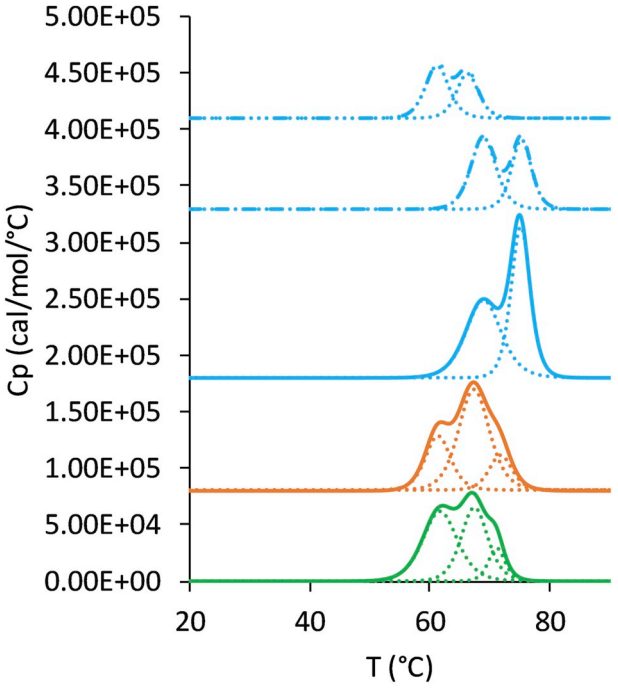

Fig. 5. DSC analysis of thermal stability of (bottom to top): BsAb1 (green), BsAb2 (orange), bivalent hu425-C_H1/C_L SEED antibody (blue full line), one-armed hu425-C_H1/C_L SEED antibody (blue dashed line), and one-armed hu425-C_H3_{KiH} SEED antibody (blue dash-dotted line). Deconvoluted thermograms are depicted in dotted lines to aid assignment of the discrete melting events to thermal unfolding of the antibody domains.

Exchanged anti-EGFR Fab domain. The second transition at T_m = 67.4 °C for BsAb1 and T_m = 67.3 °C for BsAb2 corresponds to the unfolding of the SEED-Fc fragment. The third transition at T_m = 71.1 °C for BsAb1 and T_m = 71.8 °C for BsAb2 corresponds to the unfolding of the unmodified Fab domain (anti-CD3 or anti-CD16, respectively). Together, these results show that the Domain-Exchanged Fab displayed a lower thermal stability compared to the unmodified Fab, but other domains of the BsAbs were not affected.

3.4. Functional binding activity of domain-exchanged SEED BsAbs

To test the functional activity of the binding arms of the BsAbs, binding assays to their respective targets were performed. Binding of BsAb1 (anti-EGFR C_H3_{KiH} x anti-CD3) to the EGFR-expressing A431 cell line and to CD3-positive primary human T cells was determined by flow cytometry (Fig. 6A and B). BsAb1 showed dose-dependent binding to both targets. BsAb1 bound to EGFR-positive cells with an EC_{50} of ~7 nM, which was comparable to the binding of one-armed anti-EGFR antibodies with unmodified Fab (C_H1/C_L) and with Domain-Exchanged Fab (C_H3_{KiH}) (~8 nM and ~7 nM, respectively). As expected, one-armed anti-CD3 antibody and an isotype control antibody did not bind to A431 cells (Fig. 6A). BsAb1 bound to CD3-positive primary T cells with an EC_{50} of ~37 nM. The EC_{50} for one-armed anti-CD3 antibodies with unmodified Fab (C_H1/C_L) and with Domain-Exchanged Fab (C_H3_{KiH}) was marginally higher (~50 nM). As expected, one-armed anti-EGFR and an isotype control antibody did not bind to CD3-positive primary T cells (Fig. 6B).

Binding of BsAb2 (anti-EGFR C_H3_{KiH} x anti-CD16) to CD16a was determined by a CD16a HTRF Cellular Binding assay (CisBio) (Fig. 6C). This is a competition assay that measures binding of an antibody to cell surface CD16a through a competition readout. If the antibody being tested binds to CD16a, that will reduce binding between the fluorophore-labeled cell surface CD16a and a soluble fluorophore-labeled IgG antibody standard, which in turn reduces the FRET signal measured due to interaction between the 2 labeled components of the assay. If the antibody being tested does not bind CD16a, there will be no competition observed and no reduction in the FRET signal. The relative strength of test antibody binding to CD16 can be observed and ranked with the half-maximal inhibitory concentration (IC_{50}) measured from dose-dependent competition curves.

BsAb2 can bind to CD16 *via* both the anti-CD16 Fab arm and the native FcγR-binding activity of the Fc fragment. To isolate the activity of the anti-CD16 Fab arm from the activity of the Fc portion of the BsAb to bind to FcγR (including CD16) and mediate ADCC, effector-negative versions of the BsAb and one-armed antibodies were produced. The effector-negative antibodies had their C_H2 domains replaced with an aglycosylated IgG2-C_H2 domain (designated "C_H2_{EN}"), which greatly reduces/eliminates FcγR-binding and effector functions.

As expected, no binding to CD16 was detected for the negative control effector-negative one-armed anti-EGFR antibody, as shown by the absence of competition for the FRET signal at all doses tested (Fig. 6C). BsAb2 and one-armed anti-CD16 antibody showed the strongest binding to CD16, with IC_{50} values of 0.3 and 0.1 nM. BsAb2 produced with the effector-negative variant isotype SEED-Fc_{EN} (sequence in Supplementary Table 1) ranked next in CD16 binding, with IC_{50} ~3.6 nM. One-armed anti-EGFR antibodies produced with an unmodified Fab or with a Domain-Exchanged Fab ranked in a similar and lower range of CD16 binding, with IC_{50} of 23 and 71 nM. Thus this assay ranked these antibodies into 3 categories (Fig. 6C). The sub-nanomolar IC_{50} competition range presumably represents CD16 binding from combination of both the anti-CD16 Fab binding and the native FcγR-binding activity of the Fc fragment. Competition by the effector-negative isotype BsAb2 represents only the effect of the anti-CD16 Fab binding. The weakest competition category from the one-armed anti-EGFR antibodies represents only the native FcγR-binding activity of the Fc fragment.

Altogether, these binding studies showed that the BsAbs constructed to include a Domain-Exchanged Fab had similar cognate antigen binding as their corresponding one-armed antibody variants and antigen binding was not influenced by the constant domain-exchange in a Fab fragment. Furthermore, contributions to CD16 binding in BsAb2 by the anti-CD16 Fab and the Fc domain can be combined or isolated to the anti-CD16 Fab activity, by use of IgG1-based *versus* effector-negative isotypes in the BsAb heavy chain.

3.5. Biological activity of domain-exchanged SEED BsAbs

We tested the ability of both BsAbs and their corresponding one-armed SEED antibodies to redirect effector cells to kill target cells. Activated primary T cells or NK cells were incubated with EGFR-over-expressing A431 target cells in the presence of antibodies applied in serial dilutions. Cell lysis was measured by release of the intracellular enzyme LDH.

Dose-dependent cell lysis of A431 target cells by activated T cells was measured in the presence of BsAb1 (anti-EGFR x anti-CD3) (Fig. 7A). As expected, one-armed anti-CD3, anti-CD16 and anti-EGFR C_H3_{KiH} antibodies did not induce cell lysis. In contrast, BsAb1 induced up to 50% cell lysis with a calculated EC_{50} value between 0.1 and 0.3 nM. These results demonstrate redirected T cell lysis of the target cells, which occurred only with the BsAb1 that can bind EGFR on A431 target cells with one arm and CD3 on T cells with the other arm; one-armed antibodies binding individually CD3 or EGFR did not induce target cell lysis in the presence of activated T cells.

Specific cell lysis of A431 cells by NK cells was mediated by BsAb2 and by its effector-negative variant BsAb2 SEED-Fc_{EN} (Fig. 7B). Both isotype versions of BsAb2 induced up to 50% cell lysis, however the calculated EC_{50} value determined for BsAb2 with an effector-positive IgG1-based isotype (10 pM) was lower than the EC_{50} value for BsAb2 with SEED-Fc_{EN} effector-negative isotype (37 pM). Control one-armed anti-CD3 antibody did not cause detectable lysis of target cells, as

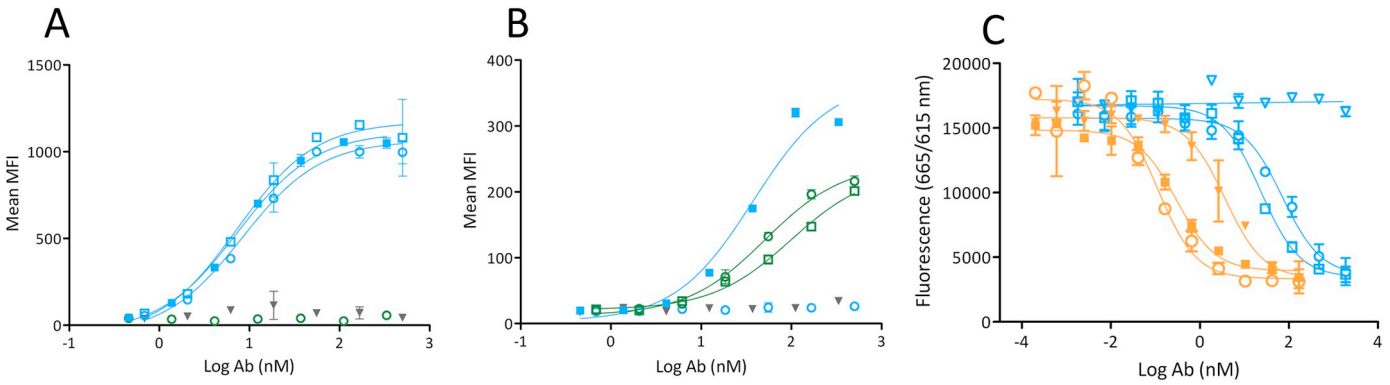

Fig. 6. Antigen-binding properties of BsAb1 and BsAb2. (A) Binding to EGFR-positive A431 cells of BsAb1 (blue full squares), one-armed hu425-C_H3_{KiH} SEED antibody (blue empty squares), one-armed hu425-C_H1/C_L SEED antibody (blue empty circles), one-armed OKT3-C_H1/C_L SEED antibody (green empty circles) and isotype control (gray triangles); (B) Binding to CD3-positive primary T cells of BsAb1 (blue full squares), one-armed OKT3-C_H3_{KiH} SEED antibody (green empty squares), one-armed OKT3-C_H1/C_L SEED antibody (green empty circles), one-armed hu425-C_H1/C_L SEED antibody (blue empty circles) and isotype control (gray triangles); (C) Binding to CD16a receptor of BsAb2 (orange full squares), effector-negative BsAb2 (orange full triangles), one-armed 3G8- C_H1/C_L SEED antibody (orange empty circles), one-armed hu425-C_H1/C_L SEED antibody (blue empty circles), one-armed hu425-C_H3_{KiH} SEED antibody (blue empty squares) and effector-negative one-armed 425- C_H3_{KiH} SEED antibody (blue empty triangles).

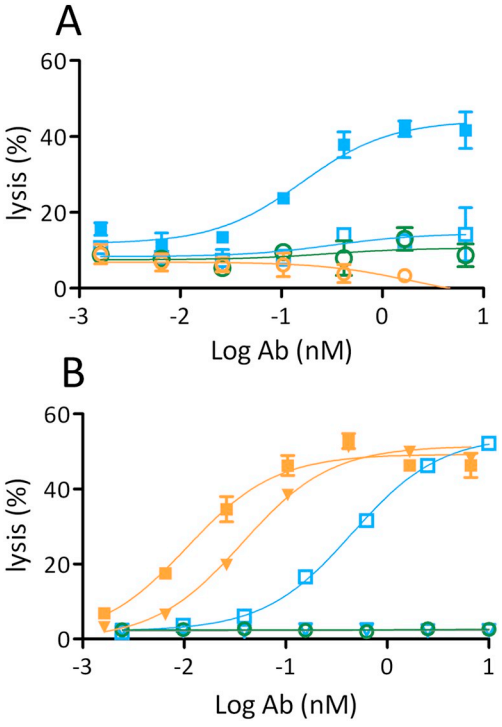

Fig. 7. Bispecific antibodies enable the immune cells to mediate target cell lysis. (A) Target cell lysis, induced with stimulated T cells in E:T ratio of 10:1. Effector cells were armed with BsAb1 (anti-EGFR-C_H3_{KiH} x anti-CD3 antibody) (blue full squares), one-armed hu425-C_H3_{KiH} SEED antibody (blue empty squares), one-armed OKT3-C_H1/C_L SEED antibody (green empty circles) or one-armed 3G8- C_H1/C_L SEED antibody (orange empty circles). (B) Target cell lysis, mediated with NK cells in an E:T ratio of 10:1. NK cells were armed with BsAb2 (anti-EGFR-C_H3_{KiH} x anti-CD16 antibody) (orange full squares), effector-negative BsAb2 (orange full triangles), one-armed hu425-C_H3_{KiH} SEED antibody (blue empty squares), effector-negative one-armed hu425- C_H3_{KiH} SEED antibody (blue empty triangles) and one-armed OKT3-C_H1/C_L SEED antibody (green empty circles). Cell lysis was measured by LDH release using CytoTox 96 Non-Radioactive Cytotoxicity Assay (Promega). Each data point is the mean ± SD of triplicates.

expected. In contrast, one-armed anti-EGFR C_H3_{KiH} SEED antibody induced up to 50% cell lysis with an EC_{50} value of ~450 pM, which represented ADCC activity mediated through the native FcγR-binding activity of the Fc domains of the one-armed anti-EGFR antibody. As expected for ADCC activity, effector-negative isotype one-armed anti-EGFR antibody did not induce target cell lysis. Thus, target cell lysis induced by effector-negative BsAb2 represented only redirected NK lysis of target cells, while effector-competent BsAb2 could induce target cell lysis both by ADCC and by redirected NK cytotoxicity.

In summary, bispecific binding to either T cells or NK cells and EGFR-expressing target cells by Domain-Exchanged SEED BsAbs redirected and activated the effector cells, resulting in potent killing of the target tumor cells.

4. Discussion

In the present work, we have explored a novel approach to govern correct heavy-to-light chain pairing in a bispecific SEED antibody by replacing constant domains in one of the Fab fragments with a pair of C_H3 domains. The specificities of the model antibodies were chosen to bridge EGFR-positive target cells with immune effector cells, either *via* CD3 or CD16a engagement in BsAb1 and BsAb2, respectively. First, we tested the feasibility of the domain exchange by expressing all three antibodies (humanized anti-EGFR, murine anti-CD3 and murine anti-CD16) as conventional and Domain-Exchanged one-armed SEED antibodies: all expressed at a similar level and exhibited sharp peaks with the area similar to their C_H1/C_L counterparts, which points towards broad applicability of this engineering method.

Full-length bispecific antibodies were expressed in mammalian cells and purified over Protein A column and size-exclusion chromatography and appeared as sharp peaks corresponding to a size of a full antibody in SEC-HPLC in native conditions. Mass spectrometry analysis of the intact BsAbs produced by co-expression of 4 protein chains detected only the heavy-chain heterodimer with one each of the different light chains, in the correct 1:1:1:1 stoichiometry of the 4 protein chains. However, mass spectrometry on the intact BsAbs could not distinguish between correctly assembled BsAbs and antibodies with light chains incorrectly swapped between the Fabs. Therefore, in a sensitive co-expression competition experiment we expressed the anti-EGFR Domain-Exchanged Fab or the anti-CD3 unmodified Fab as one-armed antibodies, while co-expressing both of the two light chains used in BsAb1. This assay tested the potential for light chain mispairing to occur among unmodified and Domain-Exchanged Fab elements under the same conditions as during expression and assembly of the BsAbs, but allowed sensitive detection of any light chain mispairing that might occur. Analysis of the one-armed antibodies produced in the co-expression competition experiments by mass spectrometry demonstrated

that > 95% correct cognate heavy-light chain pairing occurred. Homogeneity of the protein preparation allowed a comparison of antigen-binding properties of domain-exchanged antibodies with their parental version. The anti-EGFR domain-exchanged antibody bound to cell-associated cognate antigen with the same EC_{50} as the parental one-armed antibody. The binding to cell-bound antigen was not altered when the domain-exchanged Fab was incorporated into a full-length BsAb. Binding to the T cell surface of the one-armed domain-exchanged anti-CD3 antibody was comparable with its C_H1/C_L version and the BsAb with the anti-CD3-Fab. Altogether, both domain-exchanged Fab variants retained their antigen-recognition properties, similarly as described previously for the monovalent versions of the domain-exchanged antibody [42]; however in that study the very stable antibody trastuzumab was used as a scaffold.

The domain exchange caused a decrease in thermal stability of the modified Fab fragment by about 14 °C, a typical phenomenon associated with single amino acid "KiH" substitutions [46]. It is encouraging to see that the thermal stability of other domains and, more importantly, antigen binding were not adversely affected. It has been reported that alterations in antigen binding can be caused by changes in the V_H/V_L interface [51], which could also be a consequence of the domain exchange. Alterations in V_H/V_L domain association can change the shape of the antigen-binding site through modifications of the relative positions of the hypervariable loops and the positions of side chains of antigen-contacting residues [52] and *vice versa,* the modifications of amino acid residues of complementarity determining regions, in particular the V_H, can influence the framework of the variable domain and V_H/V_L association [53].

The study of binding to cell-surface expressed CD16a was designed to dissect the interaction into one mediated by the anti-CD16 antibody and one mediated by the Fc fragment. The effector-negative scaffold variant of the SEED-Fc used here was modified by replacing the C_H2 domain with an aglycosylated variant of the IgG2-C_H2 domain, and labeled as SEED-Fc_{EN}. This change eliminates or greatly reduces FcγR binding and effector functions [54–56]. The assay readout on cell surface CD16a showed the strongest CD16 binding from BsAb2 which was very similar to binding of one-armed anti-CD16 C_H1/C_L antibody. This binding was decreased by > 10-fold when the BsAb2 effector-negative isotype version was used, showing that both the anti-CD16 Fab binding site and the FcγR-binding site on the Fc domains were implicated in CD16a engagement for BsAb2 and the one-armed anti-CD16 antibody. One-armed anti-EGFR antibodies bound CD16 with only the native FcγR-binding activity of the Fc fragment, and consequently had weaker binding to CD16. This weaker level of CD16 binding was similar between one-armed anti-EGFR with an unmodified (C_H1/C_L) Fab and with a Domain-Exchanged Fab. Effector-negative isotype BsAb2 had intermediate CD16 binding that comes only from the anti-CD16 Fab. Consistent with the above results, CD16 binding was completely abrogated in the one-armed anti-EGFR antibody with the effector-negative isotype SEED-Fc_{EN}.

Finally, we tested the bispecific antibodies for their ability to induce cell-mediated lysis. BsAb1 induced potent lysis of target cells using activated T cells as effector cells, with an EC_{50} of 0.1 to 0.3 nM, which is in the range reported for other bispecific constructs involving OKT3 variable domains [57–59]. There was no target cell lysis by T cells in the presence of one-armed antibodies with the individual component Fabs of BsAb1, only when anti-EGFR and anti-CD3 were linked in a single bispecific protein. BsAb2 was tested for the ability to induce target cell lysis using NK cells as effector cells. Up to 50% lysis was induced with an EC_{50} of 10 pM. BsAb2 was more potent when the effector-competent Fc version was used, indicating that NK cell activation proceeded *via* anti-CD16 antibody and *via* the Fc fragment, and represented a combination of redirected NK target cell lysis plus ADCC. BsAb2 with effector-negative isotype still induced a similar maximum level of target cell lysis, with a relatively small increase in EC_{50}, demonstrating that redirected NK target cell lysis was very potent simply through the bispecific linkage of anti-EGFR and anti-CD16 Fabs. In contrast, the one-armed anti-EGFR domain-exchanged antibody induced specific target cell lysis only through ADCC, however with lower potency compared to BsAb2-effector-negative isotype antibody. Consistent with the CD16 binding results, one-armed anti-EGFR-effector-negative isotype antibody showed no ADCC activity and induced no target cell lysis. Together, these experiments showed the Domain-Exchanged SEED bispecific antibody format has potent biological function to redirect immune effector cells for target cell lysis.

5. Conclusions

To conclude, we have applied constant domain exchange in Fabs to address the heavy-to-light chain pairing issue in bispecific SEED antibodies. Correct assembly of the 4 co-expressed protein chains as designed was confirmed with mass spectrometry. The molecules produced by the method described herein were of favorable biophysical properties: well expressed, thermostable and dimeric in SEC under native conditions. The antigen binding properties of domain-exchanged monovalent antibodies were similar to their C_H1/C_L counterparts. The two bispecific antibodies characterized in this work acted efficiently as a bridging molecule to elicit potent target cell killing *via* redirected cytotoxicity by T cells or NK cells. In contrast to several other engineering solutions to promote specific heavy-to-light chain association, Fab constant domain exchange does not involve artificial linker sequences and appears to be applicable to several antibodies without particular optimization.

Supplementary data to this article can be found online at https://doi.org/10.1016/j.bbapap.2019.07.003.

Acknowledgements

We are grateful to Markus Windwarder, Clemens Grünwald-Gruber, Daniel Maresch and Friedrich Altmann (Glycobiology Division, BOKU, Vienna) for excellently performed MS analyses. The financial support by the Austrian Federal Ministry for Digital and Economic Affairs and the National Foundation for Research, Technology and Development is gratefully acknowledged.

Funding information

This work was supported by the Christian Doppler Research Association and the company Merck KGaA, Darmstadt, Germany. SD was also supported by the PhD program BioToP (Biomolecular Technology of Proteins) funded by the Austrian Science Fund (FWF W1224). The sponsors had no role in study design, in the collection, analysis and interpretation of data, in the writing of the report and in the decision to submit the article for publication.

Declarations of Competing Interest

Alec Gross is an employee of EMD Serono Research and Development Institute. Stefan Becker is an employee of Merck KGaA. Björn Hock is a former employee of Merck KGaA. This work is covered by a patent application WO 2016/087650.

References

[1] H. Kaplon, J.M. Reichert, Antibodies to watch in 2018, MAbs (2018), https://doi.org/10.1080/19420862.2018.1415671.

[2] S.E. Sedykh, V.V. Prinz, V.N. Buneva, G.A. Nevinsky, Bispecific antibodies: design, therapy, perspectives, Drug Des. Dev. Ther. 12 (2018) 195–208, https://doi.org/10.2147/DDDT.S151282.

[3] C. Sellmann, A. Doerner, C. Knuehl, N. Rasche, V. Sood, S. Krah, L. Rhiel, A. Messemer, J. Wesolowski, M. Schuette, S. Becker, L. Toleikis, H. Kolmar, B. Hock, Balancing selectivity and efficacy of bispecific epidermal growth factor receptor (EGFR) x c-MET antibodies and antibody-drug conjugates, J. Biol. Chem. 291 (2016) 25106–25119, https://doi.org/10.1074/jbc.M116.753491.

[4] C. Kelton, J.S. Wesolowski, M. Soloviev, R. Schweickhardt, D. Fischer, E. Kurosawa, S.D. McKenna, A.W. Gross, Anti-EGFR biparatopic-SEED antibody has enhanced combination-activity in a single molecule, Arch. Biochem. Biophys. 526 (2012) 219–225, https://doi.org/10.1016/j.abb.2012.03.005.

[5] D. Karaoglu Hanzatian, A. Schwartz, F. Gizatullin, J. Erickson, K. Deng, R. Villanueva, C. Stedman, C. Harris, T. Ghayur, A. Goodearl, Brain uptake of multivalent and multi-specific DVD-Ig proteins after systemic administration, MAbs (2018), https://doi.org/10.1080/19420862.2018.1465159.

[6] M.E. Goebeler, R. Bargou, Blinatumomab: a CD19/CD3 bispecific T cell engager (BiTE) with unique anti-tumor efficacy, Leuk. Lymphoma 57 (2016) 1021–1032, https://doi.org/10.3109/10428194.2016.1161185.

[7] U. Reusch, J. Duell, K. Ellwanger, C. Herbrecht, S.H.J. Knackmuss, I. Fucek, M. Eser, F. McAleese, V. Molkenthin, F. Le Gall, M. Topp, M. Little, E.A. Zhukovsky, A tetravalent bispecific TandAb (CD19/CD3), AFM11, efficiently recruits T cells for the potent lysis of CD19 + tumor cells, MAbs 7 (2015) 584–604, https://doi.org/10.1080/19420862.2015.1029216.

[8] U. Reusch, C. Burkhardt, I. Fucek, F. Le Gall, M. Le Gall, K. Hoffmann, S.H.J. Knackmuss, S. Kiprijanov, M. Little, E.A. Zhukovsky, A novel tetravalent bispecific TandAb (CD30/CD16A) efficiently recruits NK cells for the lysis of CD30 + tumor cells, MAbs 6 (2014) 728–739, https://doi.org/10.4161/MAbs28591.

[9] R. Linke, A. Klein, D. Seimetz, Catumaxomab: clinical development and future directions, MAbs 2 (2010) 129–136, https://doi.org/10.4161/MAbs2.2.11221.

[10] P.J. Lenting, C.V. Denis, O.D. Christophe, Emicizumab, a bispecific antibody recognizing coagulation factors IX and X: how does it actually compare to factor VIII? Blood. (2017), https://doi.org/10.1182/blood-2017-08-801662.

[11] W. Schaefer, J.T. Regula, M. Bahner, J. Schanzer, R. Croasdale, H. Durr, C. Gassner, G. Georges, H. Kettenberger, S. Imhof-Jung, M. Schwaiger, K.G. Stubenrauch, C. Sustmann, M. Thomas, W. Scheuer, C. Klein, Immunoglobulin domain crossover as a generic approach for the production of bispecific IgG antibodies, Proc. Natl. Acad. Sci. 108 (2011) 11187–11192, https://doi.org/10.1073/pnas.1019002108.

[12] L. Wang, Y. He, G. Zhang, J. Ma, C. Liu, W. He, W. Wang, H. Han, B.M. Boruah, B. Gao, Retargeting T cells for HER2-positive tumor killing by a bispecific Fv-Fc antibody, PLoS One (2013), https://doi.org/10.1371/journal.pone.0075589.

[13] C. Wu, H. Ying, C. Grinnell, S. Bryant, R. Miller, A. Clabbers, S. Bose, D. McCarthy, R.R. Zhu, L. Santora, R. Davis-Taber, Y. Kunes, E. Fung, A. Schwartz, P. Sakorafas, J. Gu, E. Tarcsa, A. Murtaza, T. Ghayur, Simultaneous targeting of multiple disease mediators by a dual-variable-domain immunoglobulin, Nat. Biotechnol. 25 (2007) 1290–1297, https://doi.org/10.1038/nbt1345.

[14] A. Steinmetz, F. Vallée, C. Beil, C. Lange, N. Baurin, J. Beninga, C. Capdevila, C. Corvey, A. Dupuy, P. Ferrari, A. Rak, P. Wonerow, J. Kruip, V. Mikol, E. Rao, CODV-Ig, a universal bispecific tetravalent and multifunctional immunoglobulin format for medical applications, MAbs (2016), https://doi.org/10.1080/19420862.2016.1162932.

[15] C. Spiess, M. Merchant, A. Huang, Z. Zheng, N.Y. Yang, J. Peng, D. Ellerman, W. Shatz, D. Reilly, D.G. Yansura, J.M. Scheer, Bispecific antibodies with natural architecture produced by co-culture of bacteria expressing two distinct half-antibodies, Nat. Biotechnol. (2013), https://doi.org/10.1038/nbt.2621.

[16] A.F. Labrijn, J.I. Meesters, B.E.C.G. de Goeij, E.T.J. van den Bremer, J. Neijssen, M.D. van Kampen, K. Strumane, S. Verploegen, A. Kundu, M.J. Gramer, P.H.C. van Berkel, J.G.J. van de Winkel, J. Schuurman, P.W.H.I. Parren, Efficient generation of stable bispecific IgG1 by controlled Fab-arm exchange, Proc. Natl. Acad. Sci. (2013), https://doi.org/10.1073/pnas.1220145110.

[17] G. Schaefer, L. Haber, L.M. Crocker, S. Shia, L. Shao, D. Dowbenko, K. Totpal, A. Wong, C.V. Lee, S. Stawicki, R. Clark, C. Fields, G.D. Lewis Phillips, R.A. Prell, D.M. Danilenko, Y. Franke, J.P. Stephan, J. Hwang, Y. Wu, J. Bostrom, M.X. Sliwkowski, G. Fuh, C. Eigenbrot, A two-in-one antibody against HER3 and EGFR has superior inhibitory activity compared with monospecific antibodies, Cancer Cell (2011), https://doi.org/10.1016/j.ccr.2011.09.003.

[18] Y. Mazor, V. Oganesyan, C. Yang, A. Hansen, J. Wang, H. Liu, K. Sachsenmeier, M. Carlson, D.V. Gadre, M.J. Borrok, X.Q. Yu, W. Dall'Acqua, H. Wu, P.S. Chowdhury, Improving target cell specificity using a novel monovalent bispecific IgG design, MAbs (2015), https://doi.org/10.1080/19420862.2015.1007816.

[19] A. Azhar, E. Ahmad, Q. Zia, M.A. Rauf, M. Owais, G.M. Ashraf, Recent advances in the development of novel protein scaffolds based therapeutics, Int. J. Biol. Macromol. 102 (2017) 630–641, https://doi.org/10.1016/j.ijbiomac.2017.04.045.

[20] W. Shatz, D. Ng, G. Dutina, A.W. Wong, D.R. Dunshee, J. Sonoda, A. Shen, J.M. Scheer, An efficient route to bispecific antibody production using single-reactor mammalian co-culture, MAbs (2016), https://doi.org/10.1080/19420862.2016.1234569.

[21] J.B.B. Ridgway, L.G. Presta, P. Carter, "Knobs-into-holes" engineering of antibody C H 3 domains for heavy chain heterodimerization, Protein Eng. 9 (1996) 617–621, https://doi.org/10.1016/1380-2933(96)80685-3.

[22] T.S. Von Kreudenstein, E. Escobar-Carbrera, P.I. Lario, I. D'Angelo, K. Brault, J. Kelly, Y. Durocher, J. Baardsnes, R. Jeremy Woods, M.H. Xie, P.A. Girod, M.D.L. Suits, M.J. Boulanger, D.K.Y. Poon, G.Y.K. Ng, S.B. Dixit, Improving biophysical properties of a bispecific antibody scaffold to aid developability: quality by molecular design, MAbs 5 (2013) 646–654, https://doi.org/10.4161/MAbs25632.

[23] K. Gunasekaran, M. Pentony, M. Shen, L. Garrett, C. Forte, A. Woodward, S. Bin Ng, T. Born, M. Retter, K. Manchulenko, H. Sweet, I.N. Foltz, M. Wittekind, W. Yan, Enhancing antibody Fc heterodimer formation through electrostatic steering effects: applications to bispecific molecules and monovalent IgG, J. Biol. Chem. 285 (2010) 19637–19646, https://doi.org/10.1074/jbc.M110.117382.

[24] H. Wei, H. Cai, Y. Jin, P. Wang, Q. Zhang, Y. Lin, W. Wang, J. Cheng, N. Zeng, T. Xu, A. Zhou, Structural basis of a novel heterodimeric Fc for bispecific antibody production, Oncotarget 1 (2017) 51037–51049, https://doi.org/10.18632/oncotarget.17558.

[25] J.H. Davis, C. Aperlo, Y. Li, E. Kurosawa, Y. Lan, K.M. Lo, J.S. Huston, SEEDbodies: fusion proteins based on strand-exchange engineered domain (SEED) CH3 heterodimers in an Fc analogue platform for asymmetric binders or immunofusions and bispecific antibodies, Protein Eng. Des. Sel. 23 (2010) 195–202, https://doi.org/10.1093/protein/gzp094.

[26] D. Skegro, C. Stutz, R. Ollier, E. Svensson, P. Wassmann, F. Bourquin, T. Monney, S. Gn, S. Blein, Immunoglobulin domain interface exchange as a platform technology for the generation of Fc heterodimers and bispecific antibodies, J. Biol. Chem. 292 (2017) 9745–9759, https://doi.org/10.1074/jbc.M117.782433.

[27] C.F. Barbas, T.A. Collet, W. Amberg, P. Roben, J.M. Binley, D. Hoekstra, D. Cababa, T.M. Jones, R.A. Williamson, G.R. Pilkington, N.L. Haigwood, E. Cabezas, A.C. Satterthwait, I. Sanz, D.R. Burton, Molecular profile of an antibody response to HIV-1 as probed by combinatorial libraries, J. Mol. Biol. 230 (1993) 812–823, https://doi.org/10.1006/jmbi.1993.1203.

[28] J. Chatellier, M.H.V. Van Regenmortel, T. Vernet, D. Altschuh, Functional mapping of conserved residues located at the VL and VH domain interface of a Fab, J. Mol. Biol. 264 (1996) 1–6, https://doi.org/10.1006/jmbi.1996.0618.

[29] A. Narayanan, B.D. Sellers, M.P. Jacobson, Energy-based analysis and prediction of the orientation between light- and heavy-chain antibody variable domains, J. Mol. Biol. 388 (2009) 941–953, https://doi.org/10.1016/j.jmb.2009.03.043.

[30] S. Portolano, G.D. Chazenbalk, P. Seto, J. Scott Hutchison, B. Rapoport, S.M. McLachlan, Recognition by recombinant autoimmune thyroid disease-derived fab fragments of a dominant conformational epitope on human thyroid peroxidase, J. Clin. Invest. 90 (1992) 720–726, https://doi.org/10.1172/JCI115943.

[31] B.J. DeKosky, T. Kojima, A. Rodin, W. Charab, G.C. Ippolito, A.D. Ellington, G. Georgiou, In-depth determination and analysis of the human paired heavy- and light-chain antibody repertoire, Nat. Med. 21 (2015) 86–91, https://doi.org/10.1038/nm.3743.

[32] N. Jayaram, P. Bhowmick, A.C.R. Martin, Germline VH/VL pairing in antibodies, Protein Eng. Des. Sel. 25 (2012) 523–530, https://doi.org/10.1093/protein/gzs043.

[33] C. Klein, C. Sustmann, M. Thomas, K. Stubenrauch, R. Croasdale, J. Schanzer, U. Brinkmann, H. Kettenberger, J.T. Regula, W. Schaefer, Progress in overcoming the chain association issue in bispecific heterodimeric IgG antibodies, MAbs 4 (2012) 653–663, https://doi.org/10.4161/MAbs21379.

[34] A.M. Merchant, Z. Zhu, J.Q. Yuan, A. Goddard, C.W. Adams, L.G. Presta, P. Carter, An efficient route to human bispecific IgG, Nat. Biotechnol. 16 (1998) 677–681, https://doi.org/10.1038/nbt0798-677.

[35] J. Jackman, Y. Chen, A. Huang, B. Moffat, J.M. Scheer, S.R. Leong, W.P. Lee, J. Zhang, N. Sharma, Y. Lu, S. Iyer, R.L. Shields, N. Chiang, M.C. Bauer, D. Wadley, M. Roose-Girma, R. Vandlen, D.G. Yansura, Y. Wu, L.C. Wue, Development of a two-part strategy to identify a therapeutic human bispecific antibody that inhibits IgE receptor signaling, J. Biol. Chem. 285 (2010) 20850–20859, https://doi.org/10.1074/jbc.M110.113910.

[36] S. Krah, C. Schröter, C. Eller, L. Rhiel, N. Rasche, J. Beck, C. Sellmann, R. Günther, L. Toleikis, B. Hock, H. Kolmar, S. Becker, Generation of human bispecific common light chain antibodies by combining animal immunization and yeast display, Protein Eng. Des. Sel. 30 (2017) 291–301, https://doi.org/10.1093/protein/gzw077.

[37] T. Van Blarcom, K. Lindquist, Z. Melton, W.L. Cheung, C. Wagstrom, D. McDonough, C. Valle Oseguera, S. Ding, A. Rossi, S. Potluri, P. Sundar, S. Pitts, M. Sirota, M. Galindo Casas, Y. Yan, J. Jones, Z. Roe-Zurz, S. Srivatsa Srinivasan, W. Zhai, J. Pons, A. Rajpal, J. Chaparro-Riggers, Productive common light chain libraries yield diverse panels of high affinity bispecific antibodies, MAbs 10 (2018) 256–268, https://doi.org/10.1080/19420862.2017.1406570.

[38] T. Igawa, H. Tsunoda, Y. Kikuchi, M. Yoshida, M. Tanaka, A. Koga, Y. Sekimori, T. Orita, Y. Aso, K. Hattori, M. Tsuchiya, VH/VL interface engineering to promote selective expression and inhibit conformational isomerization of thrombopoietin receptor agonist single-chain diabody, Protein Eng. Des. Sel. 23 (2010) 667–677, https://doi.org/10.1093/protein/gzq034.

[39] S.M. Lewis, X. Wu, A. Pustilnik, A. Sereno, F. Huang, H.L. Rick, G. Guntas, A. Leaver-Fay, E.M. Smith, C. Ho, C. Hansen-Estruch, A.K. Chamberlain, S.M. Truhlar, E.M. Conner, S. Atwell, B. Kuhlman, S.J. Demarest, Generation of bispecific IgG antibodies by structure-based design of an orthogonal Fab interface, Nat. Biotechnol. 32 (2014) 191–198, https://doi.org/10.1038/nbt.2797.

[40] Z. Liu, E.C. Leng, K. Gunasekaran, M. Pentony, M. Shen, M. Howard, J. Stoops, K. Manchulenko, V. Razinkov, H. Liu, W. Fanslow, Z. Hu, N. Sun, H. Hasegawa, R. Clark, I.N. Foltz, W. Yan, A novel antibody engineering strategy for making monovalent bispecific heterodimeric IgG antibodies by electrostatic steering mechanism, J. Biol. Chem. 290 (2015) 7535–7562, https://doi.org/10.1074/jbc.M114.620260.

[41] M. Bönisch, C. Sellmann, D. Maresch, C. Halbig, S. Becker, L. Toleikis, B. Hock, F. Rüker, Novel CH1:CLinterfaces that enhance correct light chain pairing in heterodimeric bispecific antibodies, Protein Eng. Des. Sel. 30 (2017) 685–696, https://doi.org/10.1093/protein/gzx044.

[42] G. Wozniak-Knopp, G. Stadlmayr, J.W. Perthold, K. Stadlbauer, M. Gotsmy, S. Becker, F. Rüker, An antibody with fab-constant domains exchanged for a pair of CH3 domains, PLoS One 13 (2018), https://doi.org/10.1371/journal.pone.0195442.

[43] M. Muda, A.W. Gross, J.P. Dawson, C. He, E. Kurosawa, R. Schweickhardt, M. Dugas, M. Soloviev, A. Bernhardt, D. Fischer, J.S. Wesolowski, C. Kelton, B. Neuteboom, B. Hock, Therapeutic assessment of SEED: a new engineered antibody platform designed to generate mono- and bispecific antibodies, Protein Eng. Des. Sel. 24 (2011) 447–454, https://doi.org/10.1093/protein/gzq123.

[44] G. Wozniak-Knopp, F. Rüker, A C-terminal interdomain disulfide bond significantly stabilizes the Fc fragment of IgG, Arch. Biochem. Biophys. 526 (2012) 181–187, https://doi.org/10.1016/j.abb.2012.03.024.
[45] G.M. Edelman, B.A. Cunningham, W.E. Gall, P.D. Gottlieb, U. Rutishauser, M.J. Waxdal, The covalent structure of an entire gammaG immunoglobulin molecule, Proc. Natl. Acad. Sci. U. S. A. 63 (1969) 78–85, https://doi.org/10.1073/pnas.63.1.78.
[46] S. Atwell, J.B.B. Ridgway, J.A. Wells, P. Carter, Stable heterodimers from remodeling the domain interface of a homodimer using a phage display library, J. Mol. Biol. 270 (1997) 26–35, https://doi.org/10.1006/jmbi.1997.1116.
[47] J. Schmiedel, A. Blaukat, S. Li, T. Knöchel, K.M. Ferguson, Matuzumab binding to EGFR prevents the conformational rearrangement required for dimerization, Cancer Cell 13 (2008) 365–373, https://doi.org/10.1016/j.ccr.2008.02.019.
[48] P. Kung, G. Goldstein, E. Reinherz, S. Schlossman, Monoclonal antibodies defining distinctive human T cell surface antigens, Science (80-.) 206 (1979) 347–349, https://doi.org/10.1126/science.314668.
[49] J.P. Van Wauwe, J.R. De Mey, J.G. Goossens, OKT3: a monoclonal anti-human T lymphocyte antibody with potent mitogenic properties, J. Immunol. 124 (1980) 2708–2713.
[50] B. Perussia, G. Trinchieri, Antibody 3G8, specific for the human neutrophil fc receptor, reacts with natural killer cells, J. Immunol. 132 (1984) 1410–1415.
[51] K. Masuda, K. Sakamoto, M. Kojima, T. Aburatani, T. Ueda, H. Ueda, The role of interface framework residues in determining antibody VH/VL interaction strength and antigen-binding affinity, FEBS J. 273 (2006) 2184–2194, https://doi.org/10.1111/j.1742-4658.2006.05232.x.
[52] A. Chailyan, P. Marcatili, A. Tramontano, The association of heavy and light chain variable domains in antibodies: implications for antigen specificity, FEBS J. 278 (2011) 2858–2866, https://doi.org/10.1111/j.1742-4658.2011.08207.x.
[53] E.M. Herold, C. John, B. Weber, S. Kremser, J. Eras, C. Berner, S. Deubler, M. Zacharias, J. Buchner, Determinants of the assembly and function of antibody variable domains, Sci. Rep. 7 (2017) 12276, , https://doi.org/10.1038/s41598-017-12519-9.
[54] R.L. Shields, A.K. Namenuk, K. Hong, Y.G. Meng, J. Rae, J. Briggs, D. Xie, J. Lai, A. Stadlen, B. Li, J.A. Fox, L.G. Presta, High resolution mapping of the binding site on human IgG1 for FcγRI, FcγRII, FcγRIII, and FcRn and design of IgG1 variants with improved binding to the FcγR, J. Biol. Chem. 276 (2001) 6591–6604, https://doi.org/10.1074/jbc.M009483200.
[55] M.H. Tao, S.L. Morrison, Studies of aglycosylated chimeric mouse-human IgG. Role of carbohydrate in the structure and effector functions mediated by the human IgG constant region, J. Immunol. 143 (1989) 2595–2601.
[56] M. Kinder, A.R. Greenplate, K.D. Grugan, K.L. Soring, K.A. Heeringa, S.G. McCarthy, G. Bannish, M. Perpetua, F. Lynch, R.E. Jordan, W.R. Strohl, R.J. Brezski, Engineered protease-resistant antibodies with selectable cell-killing functions, J. Biol. Chem. 288 (2013) 30843–30854, https://doi.org/10.1074/jbc.M113.486142.
[57] K. Ellwanger, U. Reusch, I. Fucek, S. Knackmuss, M. Weichel, T. Gantke, V. Molkenthin, E.A. Zhukovsky, M. Tesar, M. Treder, Highly specific and effective targeting of EGFRvIII-positive tumors with TandAb antibodies, Front. Oncol. 7 (2017) 100, , https://doi.org/10.3389/fonc.2017.00100.
[58] U. Reusch, M. Sundaram, P.A. Davol, S.D. Olson, J.B. Davis, K. Demel, J. Nissim, R. Rathore, P.Y. Liu, L.G. Lum, Anti-CD3 × anti-epidermal growth factor receptor (EGFR) bispecific antibody redirects T-cell cytolytic activity to EGFR-positive cancers in vitro and in an animal model, Clin. Cancer Res. 12 (2006) 183–190, https://doi.org/10.1158/1078-0432.CCR-05-1855.
[59] B.D. Choi, C.-T. Kuan, M. Cai, G.E. Archer, D.A. Mitchell, P.C. Gedeon, L. Sanchez-Perez, I. Pastan, D.D. Bigner, J.H. Sampson, Systemic administration of a bispecific antibody targeting EGFRvIII successfully treats intracerebral glioma, Proc. Natl. Acad. Sci. 110 (2013) 270–275, https://doi.org/10.1073/pnas.1219817110.